Magnetic island evolution in hot ion plasmas

A. Ishizawa, F. L. Waelbroeck, R. Fitzpatrick, W. Horton, and N. Nakajima

Citation: Phys. Plasmas **19**, 072312 (2012); doi: 10.1063/1.4739291
View online: http://dx.doi.org/10.1063/1.4739291
View Table of Contents: http://pop.aip.org/resource/1/PHPAEN/v19/i7
Published by the American Institute of Physics.

Magnetic island evolution in hot ion plasmas

A. Ishizawa,[1,a)] F. L. Waelbroeck,[2] R. Fitzpatrick,[2] W. Horton,[2] and N. Nakajima[1]
[1]*National Institute for Fusion Science, Toki 509-5292, Japan*
[2]*Institute for Fusion Studies, University of Texas at Austin, Austin, Texas 78712, USA*

(Received 24 February 2012; accepted 9 July 2012; published online 24 July 2012)

Effects of finite ion temperature on magnetic island evolution are studied by means of numerical simulations of a reduced set of two-fluid equations which include ion as well as electron diamagnetism in slab geometry. The polarization current is found to be almost an order of magnitude larger in hot than in cold ion plasmas, due to the strong shear of ion velocity around the separatrix of the magnetic islands. As a function of the island width, the propagation speed decreases from the electron drift velocity (for islands thinner than the Larmor radius) to values close to the guiding-center velocity (for islands of order 10 times the Larmor radius). In the latter regime, the polarization current is destabilizing (i.e., it drives magnetic island growth). This is in contrast to cold ion plasmas, where the polarization current is generally found to have a healing effect on freely propagating magnetic island. © *2012 American Institute of Physics*.
[http://dx.doi.org/10.1063/1.4739291]

I. INTRODUCTION

A. Motivation

The formation of magnetic islands degrades heat and particle confinement, limits achievable plasma beta, and can lead to plasma disruptions in high performance tokamak discharges (for a review, see Ref. 1). Magnetic islands may be caused by tearing modes, which are driven by gradients in the profile of the current density.[2] The most unstable tearing modes have long-wavelengths, and typically give rise to a small number of coherent magnetic island chains. In high-beta discharges, however, magnetic islands appear even when the linear theory of tearing modes predicts stability. Such islands are believed to result from a nonlinear instability, called the neoclassical tearing mode (NTM), that is driven by the local reduction of the bootstrap current in large islands.[3,4]

As a result of the threat that NTM present to the performance of ITER, fusion scientists have devoted intense efforts to the development of systems for their avoidance[5,6] and suppression.[7–9] Avoidance schemes focus on either eliminating or reducing the size of the magnetohydrodynamic (MHD) events, such as sawtooth crashes or edge-localized modes (ELM), that may create seed islands for the NTM. Suppression systems, by contrast, generally rely on RF waves to reverse the loss of current through a combination of heating[10] and current drive.[11] For both methods, knowledge of the critical island size for NTM growth is necessary for designing a system that will meet the needs of ITER and, in particular, for estimating the required RF power.[12]

Experiments have shown that although NTM normally require an initial seed island created during an MHD event, they also frequently grow without an observable triggering event.[13,14] A likely explanation is the formation of seed islands by turbulence. The first mechanism to be proposed for this invoked direct excitation by turbulent fluctuations.[15] A second possibility is that turbulence can induce growth indirectly by braking the island rotation, thereby producing a destabilizing polarization current.[16,17] More recently, two of us have demonstrated a third mechanism whereby ion temperature-gradient turbulence can robustly give rise to magnetic islands of size several times the ion Larmor radius, which may be sufficient to initiate NTM growth.[18] These islands are created by a process of merging, through inverse cascade, of the much smaller-scale magnetic islands that are formed as a by-product of ion temperature gradient driven (ITG) turbulence in finite-beta plasma. The possible existence of additional phenomena related to the interaction of turbulence and magnetic islands,[19] and the relative importance of the three proposed mechanisms are the subject of ongoing research.

In order to evaluate the importance of these effects for NTM control systems, it is necessary to understand better the conditions under which such islands are generated and sustained. In particular, it is necessary to know the properties of magnetic islands in the *absence* of turbulence but with finite ion temperature. Only with this knowledge can the effects of the turbulent fluctuations be quantified and understood. In particular, the size of the ITG-driven islands will depend on the balance between the rate of healing of the longest wavelength island chain and the rate of flux coalescence caused by the merging of short-scale islands. Likewise, the effect of an island chain's propagation on its width informs the effects of turbulent braking and zonal flow generation. Furthermore, the modification of the background profiles resulting from the presence of the island will control the intensity as well as the character of the turbulence.[20–22] A good understanding of the properties of islands in quiescent plasmas is thus an indispensable basis for understanding and predicting the evolution of islands in turbulent plasma.

B. Role of propagation in island evolution

The growth and healing of magnetic islands is governed by the generalized Rutherford equation

a)Electronic mail: ishizawa@nifs.ac.jp.

$$\frac{0.823}{\eta}\frac{dW}{dt} = \Delta' + \Delta_{PS} + \Delta_{bs} + \Delta_{RF} + \Delta_{\rm pol},$$

where W is the island width, η is the resistivity, and the terms on the right hand side represent the contributions from the following phenomena: the effect of the global current profile (Δ'), the Pfirsch-Schlüter current (Δ_{PS}), the bootstrap current (Δ_{bs}), the current driven by radio-frequency waves such as the ECCD (Δ_{RF}), and the polarization current ($\Delta_{\rm pol}$). Except for the polarization current (last term), the form of these contributions and, in particular, their dependence on the island width W is known.[3] In this paper, we focus on this last term. Together with the bootstrap current, the polarization current is thought to play an important role in island evolution. In particular, it is a strong candidate to explain the nonlinear threshold against the NTM, when such a threshold is observed. It may also be responsible for the initiation of the NTM in the cases when no threshold is observed.

The polarization current is caused by the acceleration of ions flowing around the magnetic island.[23] Understanding electron and ion flows around the island are thus important. Two cases must be distinguished according to whether the island chain is freely propagating or is interacting with external structures.[24] Examples of external structures include resistive walls, error fields, and resonant magnetic perturbations. The currents in such external structures exert a force on the islands, creating a momentum sink in and around the island. This results in global changes in the velocity profile. In the case of free propagation, by contrast, the modification of the plasma rotation profile caused by the presence of the island is localized to the close vicinity of the island. In the present paper, we will examine the general case in Sec. III, before specializing to the case of free propagation in Sec. IV.

Early investigations of the evolution of island propagation in the presence of finite ion and electron drifts used hypothetical profiles for the electrostatic potential.[23,25,26] In a series of papers, Fitzpatrick and collaborators subsequently showed how to solve the momentum transport equation in the island in order to determine the profiles and the propagation velocity self-consistently, considering consecutively the effects of ion viscosity,[27] electron viscosity,[28] external forces,[29] Reynolds stresses,[30] and emission of drift-acoustic waves.[31]

A central consideration when evaluating the velocity profile is the degree of flattening of the density profile. The flattening, which is due to sound wave propagation, occurs when the sound wave frequency becomes comparable to or greater than the drift frequency.[32] This corresponds to island widths $W \sim \rho_s L_s/L_n$, where L_s and L_n are the shear and density gradient lengths, respectively,[32] and $\rho_s = c_s/\omega_{ci}$ is the ion-sound Larmor radius. Here $c_s = \sqrt{T_e/m_i}$ and $\omega_{ci} = eB_0/m_i$ are the sound speed and the cyclotron frequency, respectively. Note that in the absence of curvature drifts, the electron and ion fluid velocities consist of the $E \times B$ velocity V_E and the diamagnetic velocities V_{*i} and V_{*e}. As a result of the local reduction of the diamagnetic velocity caused by the flattening, the diamagnetic velocities vary rapidly (i.e., over a scale short compared to the island width) across the separatrix of a large magnetic island.[28–30]

In the subsonic regime ($c_s \gg V_*$, or equivalently $W \gg \rho_s L_s/L_n$), where the profiles are completely flattened, analytic estimates of the polarization contribution take the form[29]

$$\Delta_{\rm pol}(V) = \frac{L_s^2}{V_A^2}\left[1.4\frac{(V_0 - V_E)(V_0 - V_i)}{(W/4)^3} - 0.4\frac{(V_0 - (V_E + V_i)/2)V'_\infty}{(W/4)^2} + 0.5\frac{V'^2_\infty}{(W/4)}\right], \quad (1)$$

where V'_∞ is the asymptotic velocity gradient (proportional to the external force acting on the island), V_0 is the island propagation velocity, V_E is the electric drift velocity, $V_i = V_{*i} + V_E$ is the ion perpendicular velocity, and V_A is the Alfvén velocity. This analytic result shows that the polarization current is a quadratic function of the island velocity as well as the external force. It also shows the importance of finite ion temperature, as well as the need for determining the island propagation velocity in order to evaluate the effect of polarization currents on island evolution. In the presence of both ion and electron viscosity (respectively, μ_i and μ_e), the propagation velocity in this regime is

$$V_0 = \frac{\mu_i V_i + \mu_e V_e}{\mu_i + \mu_e}. \quad (2)$$

That is, the competition between electron and ion viscosity governs the propagation velocity. In particular, when the ion dominates the electron viscosity, the island propagates at the background (i.e., unperturbed) ion drift velocity.

An important implication of Eqs. (1) and (2) is that for freely propagating islands in the subsonic regime, the polarization current vanishes for $\mu_e \ll \mu_i$. Since external forces are small for small islands ($V' \sim V_E/L$, where $L \gg W$ measures the plasma size), the stabilization threshold for NTM depends on sonic effects, i.e., on *departures* from Eq. (1). One source of such departures is the generation of zonal flows by the Reynolds stress, which causes $\Delta_{\rm pol}$ to peak in the sonic regime ($k_\| c_s \sim k_y V_*$).[36] Since the Reynolds stress vanishes when the electric field vanishes, the theory of Refs. 30 and 37 predicts that in the sonic regime the island propagates between the guiding center and the background (unperturbed) *ion* velocity. For large islands ($W \sim 40\rho_s$), this is in agreement with experimental observations[33] and with numerical results.[30,34]

For intermediate-size islands ($W/\rho_s \sim 5 - 10$) comparable to the observed "seed" islands for NTM, however, the propagation frequency and the polarization current are still poorly understood. Analytically, such islands fall between the hypersonic and sonic regimes of Ref. 37. The transition between these two regimes has only been investigated numerically in the limit of cold ions.[36] In the transitional range corresponding to intermediate island widths, there is a need for an improved understanding of competition between (i) viscous momentum transport, (ii) Reynolds stress, (iii) the radiative forces, and (iv) partial density and temperature flattening. In the present paper, we reexamine the problem of island propagation with finite ion drifts in order to shed light on the relative importance of these various effects. We do this by

numerically solving a reduced two-fluid model including both electron and ion diamagnetic effects.[35] In order to better understand the balance of forces that determines the island growth and decay as well as its propagation velocity, we restrict the simulations to the electrostatic limit in which both the propagation velocity and island size are fixed.[16,36] This makes it possible to chart the plasma response systematically. We note that electromagnetic simulations, in which the island is allowed to evolve "self-consistently" according to the dynamical equations, are limited by the fidelity of the model for the other types of currents entering into the generalized Rutherford equation, such as the bootstrap current, RF-driven currents, etc. Rather than chronicling the evolution of islands for a particular model, our goal here is to determine the functional dependence of $\Delta_{\rm pol}(W, V_0)$.

The paper is organized as follows. In Sec. II, we describe the reduced two-fluid equation and the electrostatic formulation. In particular, we describe the specification of the island propagation in terms of the boundary conditions and explain how we evaluate the drag force and the polarization current term. We next present the simulation results for dragged magnetic island in Sec. III. In Sec. IV, we examine the special case of freely propagating magnetic island. Last, we summarize our results in Sec. V.

II. MODEL EQUATIONS AND NUMERICAL SETTINGS

A. Formulation

We consider a two-dimensional slab plasma which is uniform along an ambient magnetic field. The model used here is a reduced set of two-fluid equations.[18,35] The model consists a set of equations that describes temporal evolutions of the electrostatic potential Φ, the density n, the parallel ion velocity $v_\parallel$, and the ion temperature T_i. In keeping with our electrostatic approach, we neglect the rate of growth of the island in the electron parallel momentum equation (Ohm's law). This is justified for tearing modes with poloidal mode number $m \neq 1$ for which the growth is much slower than the relaxation of the profiles in the magnetic island. In this context, Ohm's law serves to determine the parallel component of current density J.

The equations are

$$\frac{\partial \nabla_\perp^2 \Phi}{\partial t} = -[\Phi, \nabla_\perp^2 \Phi]/\rho_* + \beta[\psi, J]/\rho_* + \tau_i \nabla_\perp \cdot [\nabla_\perp \Phi, p_i]/\rho_* + \mu \nabla_\perp^4 (\Phi + \tau_i p_i), \tag{3}$$

$$\frac{\partial n}{\partial t} = -[\Phi, n]/\rho_* + \beta[\psi, J]/\rho_* + \beta[\psi, v_\parallel]/\rho_* + \mu_n \nabla_\perp^2 n, \tag{4}$$

$$\frac{\partial v_\parallel}{\partial t} = -[\Phi, v_\parallel]/\rho_* + \beta(1+\tau_i)[\psi, n]/\rho_* + \beta\tau_i[\psi, T_i]/\rho_* + \mu_v \nabla_\perp^2 v_\parallel, \tag{5}$$

$$\eta J = -\beta[\psi, \Phi]/\rho_* + \beta[\psi, n]/\rho_*, \tag{6}$$

$$\frac{\partial T_i}{\partial t} = -[\Phi, T_i]/\rho_* + (\Gamma - 1)\beta[\psi, v_\parallel]/\rho_* - \tau_i(\Gamma - 1)\kappa_L T_i + \mu_T \nabla_\perp^2 T_i, \tag{7}$$

where $f = f_{eq} + \rho_* \tilde{f}$, $\psi = \psi_{eq} + \rho_* \tilde{\psi}$, $\Phi = (\tilde{\phi} + \tilde{\phi}_b)\rho_*$, $n = n_{eq} + \rho_* \tilde{n}$, $v_\parallel = \rho_* \tilde{v}_\parallel$, $p = p_{eq} + \rho_* \tilde{p}$, $T_i = T_{ieq} + \rho_* \tilde{T}_i$, $\tilde{p} = \tilde{p}_i + \tilde{p}_e$, $\tilde{p}_i = \tilde{n} + \tilde{T}_i$, $\tilde{p}_e = \tilde{n}$, $\rho_* = \rho_s/L_x$, $\kappa_L = \sqrt{\frac{8T_{i0}}{\pi}}|\nabla_{\parallel eq}|$, $L_n = 1/\rho_*$. The equations include not only electron diamagnetic effects in the Ohm's law Eq. (6), but also ion diamagnetic effects in the vorticity equation Eq. (3), where the electron and ion diamagnetic velocities are $\mathbf{V}_{de} = -\mathbf{e}_z \times \nabla n$ and $\mathbf{V}_{di} = \tau_i \mathbf{e}_z \times \nabla p_i$, respectively. Velocities are normalized by the equilibrium part of electron diamagnetic velocity $V_{*e} = 1/L_n$ in figures. Cartesian coordinates (x, y, z) are adopted. The normalizations are $(tc_s/L_n, x/\rho_s, y/\rho_s, e\Phi/T_{e0}, \psi/\beta B_0 \rho_s, n/n_0, v_\parallel/c_s, T_i/T_{e0}) \to (t, x, y, \Phi, \psi, n, v_\parallel, T_i)$. Here, the density gradient scale length L_n is taken as the system size, $\tau_i = T_i/T_e$ is the ratio of ion and electron temperatures, $\beta = 4\pi n_0 T_{e0}/B_0^2$ is the electron beta, μ, η, μ_n, μ_v, and μ_T are the viscosity, the resistivity, diffusion coefficients of the density, the parallel ion velocity, and ion temperature, respectively. The operator $[f, g]$ denotes the Poisson bracket, $[f, g] = \mathbf{e}_z \cdot \nabla_\perp f \times \nabla_\perp g$, where the perpendicular components of a partial differential operator is represented as $\nabla_\perp = \mathbf{e}_x \partial_x + \mathbf{e}_y \partial_y$.

We assume a uniform equilibrium current density and use the constant-ψ approximation. Accordingly we represent the magnetic flux by

$$\psi = \psi_{eq}(x) + \rho_* \Psi \cos k_{y1} y,$$

where $\psi'_{eq} = \epsilon x/(\beta L_s)$, $k_{y1} = k_y(k=1) = 2\pi/L_y$ and the size of the magnetic island is fixed, i.e., Ψ is constant. The width of island is given by $W = \sqrt{16\Psi\rho_*\beta L_s/\epsilon}$. The density and temperature gradients are $n'_{eq} = -1/L_n$ and $T'_{ieq} = -1/L_T$. In order to avoid ion temperature gradient instabilities, the temperature gradient is set to be zero, $\eta_i = L_n/L_T = 0$ in this paper.

We introduce a background E × B flow by imposing a potential difference across the simulation region. From $\mathbf{V}_E = \mathbf{e}_z \times \nabla\Phi$, it is easy to see that this potential difference is proportional to the total flux of plasma $\Gamma = \int V_{Ey}\, dx$ through the simulation region. We parametrize the flux by the corresponding unperturbed velocity $u_b = \partial\tilde{\phi}_b/\partial x$, where $\tilde{\phi}_b = u_b x$ is the background electrostatic potential. A result of the choice of constant-flux boundary conditions is that any braking of the plasma in the neighborhood of the island must be accompanied by an increase in the velocity away from the island. We also require $\nabla^2\Phi = 0$ at the boundary, corresponding to a free-slip boundary (i.e., no diffusive momentum flow through the boundary). This last choice is mainly a matter of numerical convenience. In most confinement devices, there is a large diffusive momentum flux through the boundary. The momentum flows near the island, however, are independent of the nature of the momentum source or sink at large distances, so that the *local* properties of the island are the same for a continuously distributed momentum source or for a remote momentum sink such as a limiter or divertor.

We briefly describe the code used in this work. This code applies a finite-difference method in the radial direction x and a Fourier decomposition with poloidal mode number k

in the poloidal direction y. It evaluates the nonlinear terms with a pseudo spectral method.[35] The time-advance uses the fourth-order Runge-Kutta method with the time step width $\Delta t = 1 \times 10^{-4}$. All the simulations shown in this paper use $N_x = 128$ grid-points for the radial direction and $N_y = 40$ poloidal modes. The domain of the numerical simulations is $x = [0, L_x]$ and $y = [0, L_y]$, where $L_y = 4L_x$ and $L_x = L_n$. The scale lengths of magnetic shear and density gradient are $L_s/\epsilon = 120$ and $L_n = 1/\rho_* = 40$, respectively. The default parameters are $\eta/\beta = 0.1$, $\beta = 0.01$, $\mu = \mu_n = \mu_v = \mu_T = 0.1$.

B. Force balance and polarization current term

Here, we describe the balance of forces acting on the islands, and the polarization current term in the Rutherford equation. The poloidal component of the momentum conservation equation, averaged over the entire simulation volume, is

$$\frac{d\bar{v}_y}{dt} = F_y + \Theta_y, \tag{8}$$

where $v_y = \partial_x \Phi$ is the poloidal velocity,

$$\bar{v}_y = \int_0^{L_x} \frac{dx}{L_x} \int_0^{L_y} \frac{dy}{L_y} v_y,$$

is the volume-averaged poloidal velocity,

$$F_y = -\beta \rho_* \int_0^{L_x} \frac{dx}{L_x} \int_0^{L_y} \frac{dy}{L_y} \tilde{J} \partial_y \tilde{\psi},$$

is the electromagnetic force acting in y direction, and Θ_y is the external force responsible for the E × B flow, u_b. In a linear experiment the external force could be imposed either by biasing or by an axial (along $\mathbf{e}_z$) pressure gradient, while in a toroidal experiment it could correspond to neutral beam injection (NBI). Note that we have used the free-slip boundary condition to eliminate the viscous force from Eq. (8).

In steady state, the force acting on the magnetic island is $\Theta_y = -F_y$. Since the island is thin compared to the simulation box, most of the momentum is injected outside the island and viscously transported into the island region. We remark that the figures in Sec. III show $\hat{F}_y = F_y L_x L_y/(2\pi\beta) = F_y/(\beta\rho_*^2\pi/2)$ as a function of the velocity normalized by the electron drift velocity $u = u_b/V_{*e}$.

Since the interaction forces between a magnetic island and external structures is generally small in a nominally axisymmetric device, the average plasma velocity in islands propagating freely, defined by

$$F_y(u_{\text{free}}) = 0,$$

is of particular interest. The dependence of u_{free} on the other parameters is the subject of Sec. IV. Note that the propagation velocity of the island in a frame where the background plasma is at rest is equal and opposite to the plasma velocity away from the island in the rest frame of the island. For sufficiently large simulation domains, the background velocity is close to the average velocity, so that $V_{\text{island}}/V_{*e} = -u$.

The effect of the polarization current on the island evolution is measured by the parameter Δ_{pol}, here given by

$$\Delta_{\text{pol}} = -\frac{1}{\beta\Psi} \int_0^{L_x} \frac{dx}{L_x} \int_0^{L_y} \frac{dy}{L_y} \tilde{J} \cos k_{y1} y.$$

In Sec. III, we will investigate the dependence of this parameter on the injected momentum (parametrized by u) and on the island width.

III. FORCED ISLAND PROPAGATION

In order to clarify the effects of finite ion temperature, we consider three cases. The first is referred to as the "incompressible" case because it neglects parallel velocity, which accounts for the leading-order term in $\nabla \cdot \mathbf{v} \simeq \nabla_\parallel v_\parallel$. For this case, we solve Eqs. (3), (4), (6), and (7). Except for the evolution of the ion temperature, this case is analogous to the simulations in Ref. 17. The second is referred to as the "cold ion" case. This case neglects ion temperature, $\tau_i = 0$, i.e., it neglects the ion diamagnetic term in the vorticity equation and the ion pressure in the parallel velocity equation and solves Eqs. (3)–(6), which are the same as those used in the simulations in Ref. 36. The third and last case, corresponding to a hot ion plasma, solves Eqs. (3)–(7) with $\tau_i = 1$. This last case differs from the simulations of Ref. 34 and from the simulations of Ref. 30 having negligible electron viscosity in two ways. First, it includes the evolution of the ion temperature, and second, it neglects the inductive electric field.

A. Incompressible plasma

First, we consider incompressible plasma by neglecting the parallel velocity. Figure 1 shows that F_y and the polarization current Δ_{pol} vanish together at $u = u_{\text{free}} = -1$. This corresponds to an island that is co-propagating with the electrons, so that $\Phi = n = -x/L_n$, which leads to parallel force-balance for the electrons, $\nabla_\parallel(\Phi - n) = 0$. The current density thus vanishes ($J = 0$), since the applied $E \times B$ flow totally cancels out the equilibrium electron diamagnetic flow, resulting in $F_y = 0$ and $\Delta_{\text{pol}} = 0$.[17]

The force F_y is proportional to $u_{\text{free}} - u$, with a proportionality constant that increases with the island width. The curves of Δ_{pol}, by contrast, resemble parabolas, consistent with Eq. (1). In addition to their common zero at $u = -1$, the curves have a second root for $\Delta_{\text{pol}}(u) = 0$ at $u > -1$. For $W = 6.9\rho_s$, however, the curve of Δ_{pol} differs significantly from the others. In particular, the first root of $\Delta_{\text{pol}} = 0$ at $u = -1$ appears to be a double root, while another root lies at some $-1 < u < 0$. Since $\Delta_{\text{pol}} > 0$ for large velocities ($u \gg 1$), we expect that yet another root exists at larger values of u. The structure of the Δ_{pol} curve for this value of the island width may be related to the oscillation due to drift waves observed in Ref. 17, although here the force curve is much smoother due to the higher values of viscosity and diffusivity in our simulations. When the width of the simulation box is smaller and closer to the island width, however,

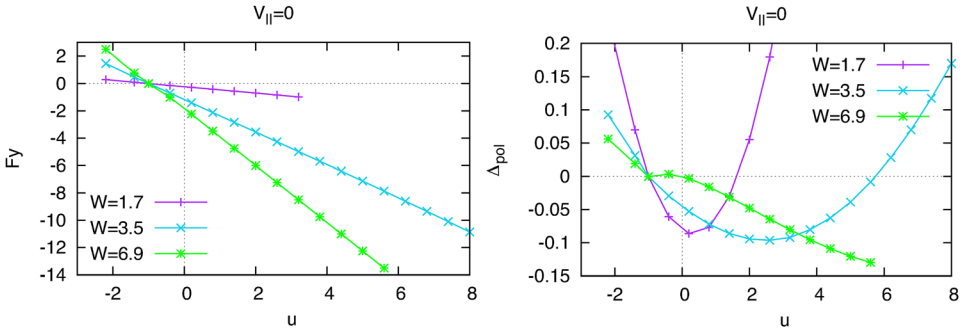

FIG. 1. Electromagnetic force and polarization current in incompressible plasma $v_{\parallel} = 0$.

the force curve does exhibit structure similar to that in Ref. 17, such as additional roots for $F_y = 0$ between $u = -1$ and 0.

Figure 2 shows the profiles of the total ion velocity $V_{iy} = V_{Ey} + V_{diy}$ and of the electron diamagnetic velocity V_{dey} on the line $y = L_y/2$ passing through the O-point of the magnetic island, for $W/\rho_s = 3.5$ and 6.9, where $V_{Ey} = \partial_x \Phi$, $V_{diy} = \tau_i \partial_x p_i$, and $V_{dey} = -\partial_x n$ Comparison of the profiles for the two island widths show that as the island width increases with respect to ρ_s, the ions inside the separatrix are increasingly constrained to flow at some fixed, "natural" velocity regardless of the forced flow. For the parameters of this simulation, the natural ion velocity lies slightly above -2. The $u = -1$ line indicates the profile $V_{iy}/V_{*e} = -2$ corresponding to the solution $\Phi = n = -x/L_n$. For this solution, $V_{Ey}/V_{*e} = u = -1$, $V_{diy}/V_{*e} = -1$, and $V_{ey} = V_{Ey} + V_{dey} = 0$. This flat profile implies there is no velocity shear, and thus both the force acting on the island and the polarization current vanish: $F_y = \Delta_{\rm pol} = 0$. In the cases with $u < -1$, $d^2 V_{iy}/dx^2 < 0$ in the island region, indicating that the viscous force acting on the island is negative, consistent with the fact that it must balance the positive electromagnetic force ($F_y > 0$). Away from the island region, by contrast, the viscous force changes sign as it must balance the external force Θ_y (e.g., the neutral beams). In the cases with $u > -1$, by contrast, all the above signs are reversed although there are some oscillations in $d^2 V_{iy}/dx^2$ that suggest that some momentum is being transported by drift waves.

B. Cold ion plasmas

Next, we include the parallel velocity and consider compressible plasma with cold ions (Fig. 3). In compressible plasma, the sound wave propagation flattens the density inside the island,[32] so that the equilibrium electron diamagnetic flow is locally reduced. For $W = 3.5\rho_s$, this flattening is small so that the average free-flow velocity remains close to -1. The wider the island, however, the stronger the flattening, so that $u_{\rm free}$ increases to -0.8 for $W = 6.9\rho_s$ and about -0.7 for $W = 9.8\rho_s$. The force F_y is again proportional to $u_{\rm free} - u$, with a proportionality constant that increases with the island width.

The curves of the polarization current integral $\Delta_{\rm pol}$ show that there are two roots for $\Delta_{\rm pol}(u) = 0$ that bound the region where the polarization drift is stabilizing. One is at $u < -1$, and the other is at $u > 0$. The polarization current term at $u = u_{\rm free}$ is negative, $\Delta_{\rm pol} < 0$, for all island widths. This means that the flattening of density due to the sound wave propagation within the island gives the polarization current a healing influence in cold-ion plasma. This is consistent with previous results.[36] We note that a difference with the results for the incompressible case is the dependence of the

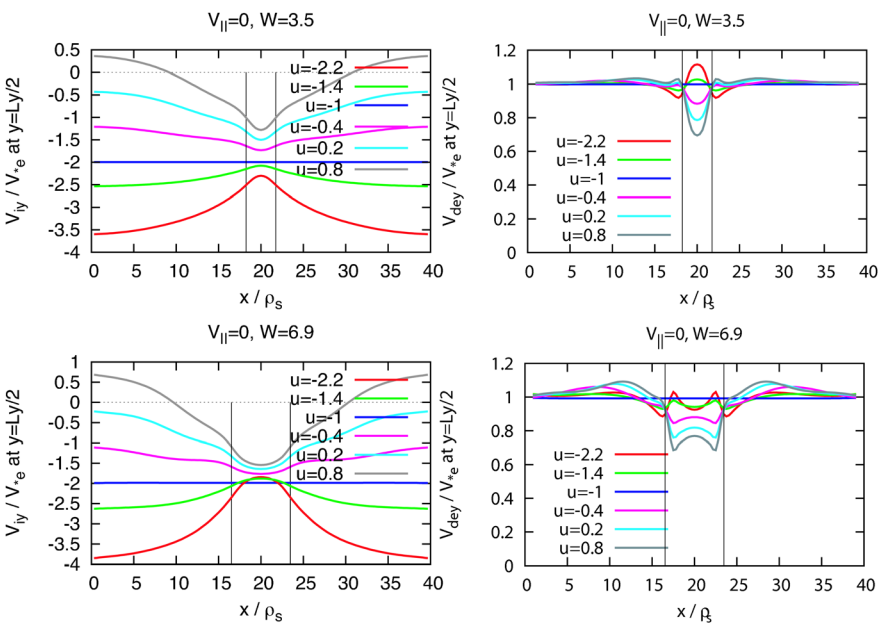

FIG. 2. Ion velocity profile $V_{iy} = V_{Ey} + V_{diy}$ and electron diamagnetic velocity profile V_{dey} in incompressible plasma on the line passing through the O-point $y = L_y/2$ for $W/\rho_s = 3.5$ and 6.9. Vertical lines indicate the separatrix of magnetic island.

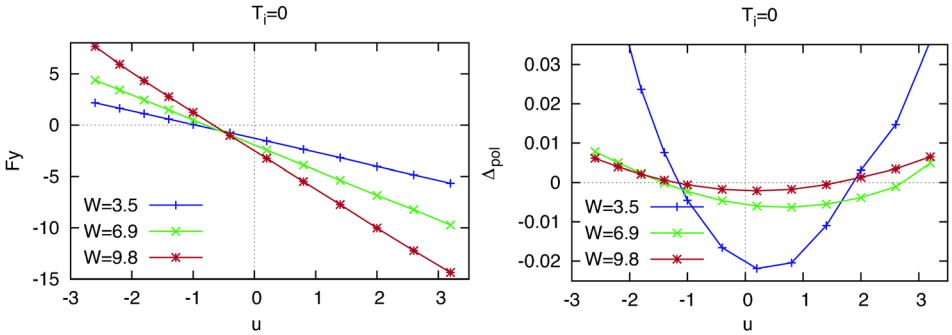

FIG. 3. Electromagnetic force and polarization current in cold ion plasma $T_i = 0$.

polarization current on the island width W. While in the incompressible case $\Delta_{\rm pol}$ increases with W, in the compressible case, it decreases with W.

Figure 4 shows the total ion velocity and the electron diamagnetic velocity profiles on the line $y = L_y/2$ passing through the O-point of the magnetic island for $W/\rho_s = 3.5$, 6.9, and 9.8. Note that for $T_i = 0$, $V_{iy} = V_{Ey}$. As the island width increases, the ion velocity inside the separatrix seems increasingly drawn to zero, regardless of the amplitude of the forced flow and despite the incomplete flattening. The plasma near the separatrix, however, is impelled in the ion direction regardless of the direction of flow outside the separatrix. For $u = 0.8$, for example, the ion velocity at the separatrix is near $V_{iy} = -0.5$ for $W/\rho_s = 9.8$. For large island width, the density gradient nearly vanishes at the O-point but rises rapidly towards the separatrix. Note that the curvature of the velocity profile away from the island is proportional to F_y, since far from the separatrix the Maxwell and Reynolds stresses become negligible and the viscous force must balance the momentum source. The profile corresponding to free propagation can therefore be identified as that for which the curvature (second derivative) of the velocity profile vanishes far from the separatrix. For this profile, the average velocity $u = u_{\rm free}$ is approximately equal to the asymptotic velocity at large distances, partly because of the small size of the island compared to the averaging domain, and partly because of the mildness of the variation of the velocity in the island region for free islands.

C. Hot ion plasmas

We next consider the complete model given by Eqs. (3)–(7), including the effects of hot ions as well as both parallel flow and ion diamagnetism ($\tau_i = 1$).

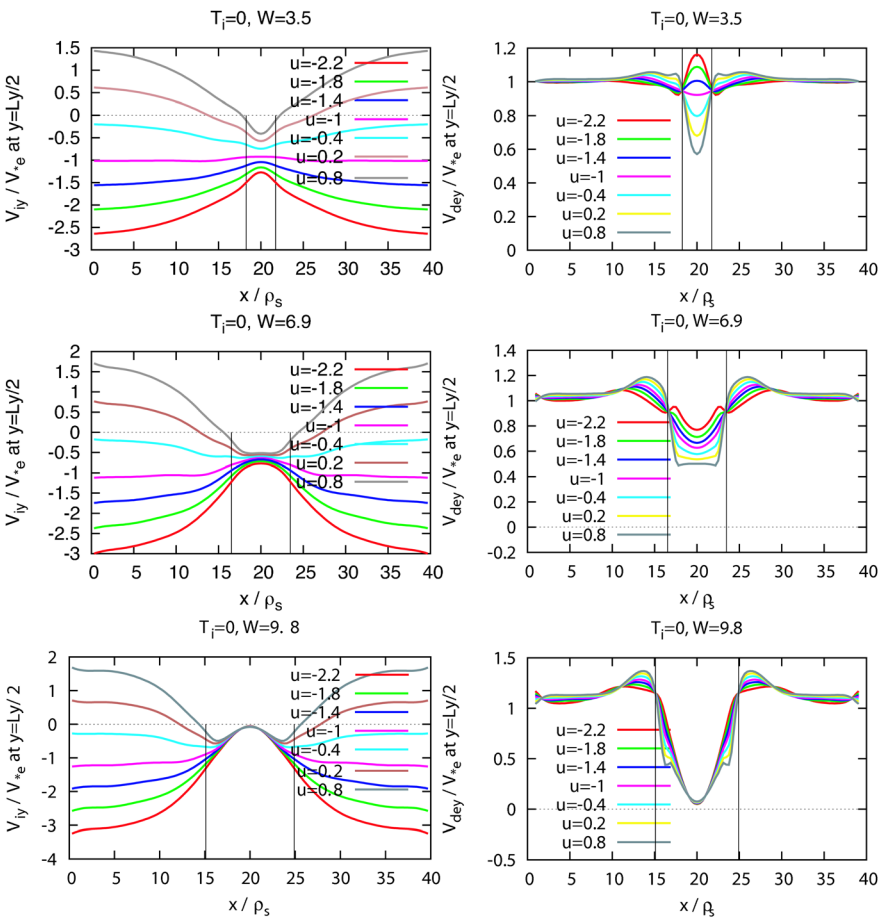

FIG. 4. Ion velocity profile $V_{iy} = V_{Ey}$ and electron diamagnetic velocity profile V_{dey} in cold ion plasma on the line passing through the O-point $y = L_y/2$ for $W/\rho_s = 3.5$, 6.9, and 9.8. Vertical lines indicate the separatrix.

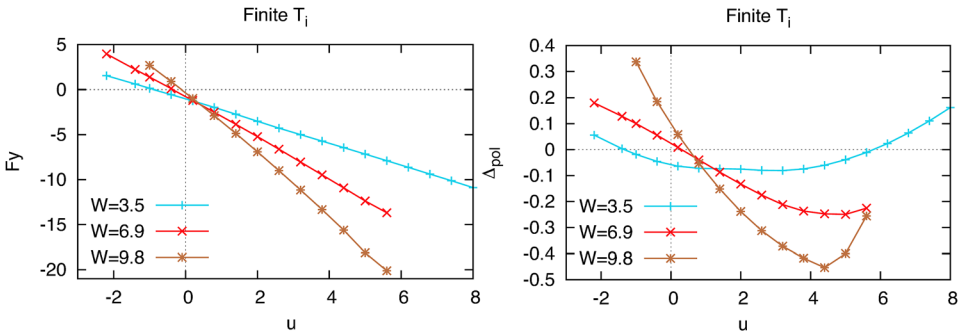

FIG. 5. Electromagnetic force and polarization current in hot ion plasma.

Figure 5 shows the force and polarization current. For $W = 3.5\rho_s$, $u_{\rm free}$ is still close to -1. As the island width becomes large, $u_{\rm free}$ increases faster than for the cold-ion case, such that $u_{\rm free} = -0.35$ for $W = 6.9\rho_s$ and $u_{\rm free} = -0.1$ for $W = 9.8\rho_s$. The increase of $u_{\rm free}$ is mainly due to the profile flattening within the island separatrix. The force remains proportional to $u_{\rm free} - u$, as for the cold ions and incompressible cases. We remark that we do not include the equilibrium part of the ion temperature gradient, $\eta_i = 0$, in order to avoid ion temperature gradient instabilities, but include the fluctuating part of the ion temperature. The ion diamagnetic flow thus includes perturbation-induced temperature gradient drifts in addition to the density gradient drifts.

In Fig. 5, we expect to find two roots for $\Delta_{\rm pol}(u) = 0$, as we have seen for cold ion plasmas. For $W = 3.5\rho_s$, the upper root is larger than 4 while the lower root lies between -1 and 0. For larger island $W = 6.9\rho_s$ and $9.8\rho_s$, the lower root becomes positive. The shift of the roots of $\Delta_{\rm pol}(u) = 0$ to more positive values as the island width grows is consistent with analytic results. Surprisingly, the polarization current for hot ion plasmas is much larger than that for cold ion plasmas. This is related to the form of the velocity profiles, which we consider next.

Figure 6 shows total ion velocity $V_{iy} = V_{Ey} + V_{diy}$ and the ion diamagnetic velocity V_{diy} profiles on the line passing through the O-point of the magnetic island $y = L_y/2$ for $W/\rho_s = 3.5$, 6.9, and 9.8. Note that for $W = 9.8\rho_s$, the diamagnetic flow almost vanishes at the O-point ($x = 20\rho_s$). As in the compressible cold-ion case, the velocity profiles exhibit structure around the separatrix even when $F_y = 0$,

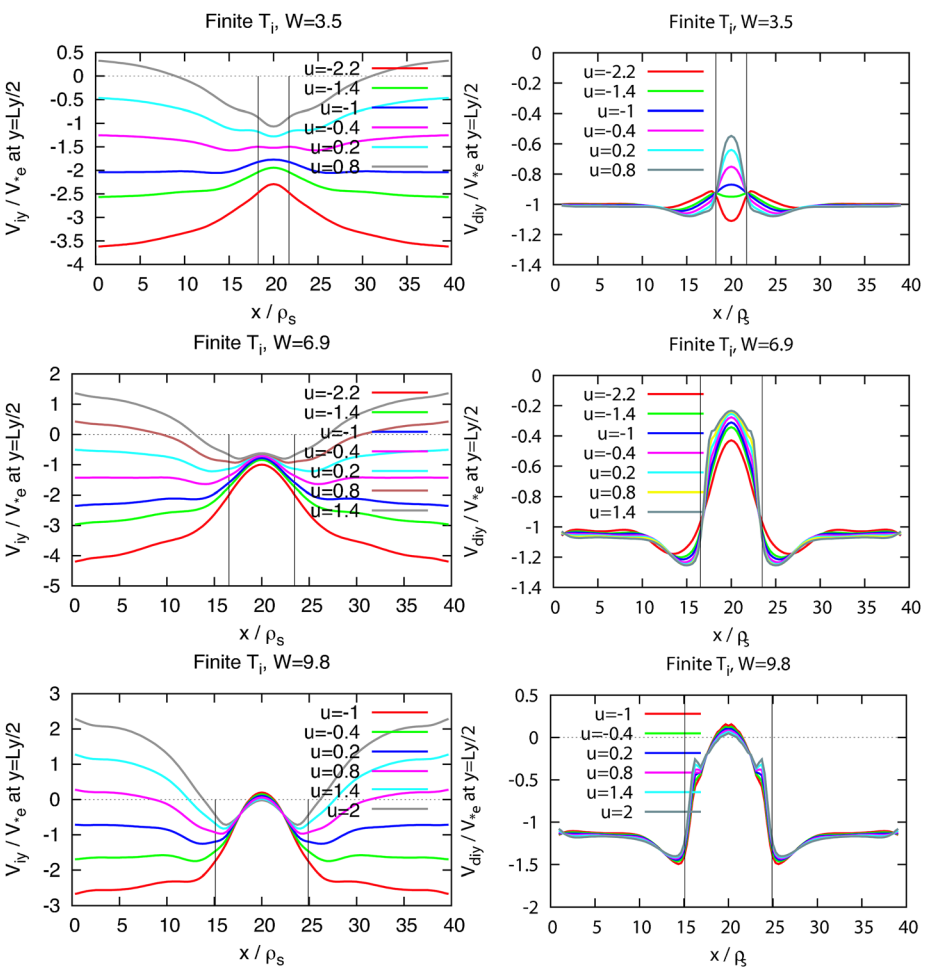

FIG. 6. Ion velocity profile $V_{iy} = V_{Ey} + V_{diy}$ and ion diamagnetic velocity profile V_{diy} in hot ion plasmas on the line passing through the O-point $y = L_y/2$ for $W/\rho_s = 3.5$, 6.9, and 9.8. Vertical lines indicate the separatrix.

reflecting local momentum transport within the island region that could be due to either the Reynolds stress or to the emission and reabsorption drift-acoustic waves. The velocity gradients around the separatrix are larger than in the cold ion case, accounting for the large $\Delta_{\rm pol}(u)$ shown in Fig. 5. The tendency of the plasma near the separatrix to rotate in the ion drift direction is also stronger than for cold ions.

D. A model of $\Delta_{\rm pol}$

We may summarize the results of the present section in terms of the following model suggested by our numerical results as well as the analytic result in Eq. (1):

$$\Delta_{\rm pol} = A(W)(u - u_-(W))(u - u_+(W)), \tag{9}$$

where $A(W)$ is a coefficient and u_+ and u_- describe the bounds of the stabilizing region. Note that u plays a role analogous to that of V'_∞ in Eq. (1). Analogues to $u_\pm$ may be computed in terms of V_i and V_e from Eq. (1), but the differences in the boundary conditions used here disallow any quantitative comparison. Table I shows $C_{\rm pol}$, u_+, and u_- for the cold and hot ion plasmas. In the case of cold ions, the following model describes the variation of the parameter $A(W)$:

$$A(W) = \frac{C_{\rm pol}}{W(W^2 + W_c^2)},$$

where $C_{\rm pol} = 1.5$ and the critical island width W_c is about $7\rho_s$. This model is qualitatively consistent with analytic results in the limits of large as well as small islands. For hot ions, on the other hand, $A(W)$ increases with W so that the dependence of $\Delta_{\rm pol}$ differs qualitatively from the cold-ion result.

IV. NATURAL ISLAND PROPAGATION

In this section, we focus our attention on the important special case of free propagation, where the external force acting on the magnetic island vanishes. In particular, we examine the dependence of the polarization integral on the island width. We identify the average flows $u_{\rm free}$ corresponding to free rotation by interpolation from the curves $F_y(u)$ in Figs. 1, 3, and 5. Recall that, as noted in Sec. II B, for *freely propagating* islands, the average velocity $u_{\rm free}$ is, to a good approximation, equal to the asymptotic electric drift velocity away from the island, which is itself equal and opposite to the normalized island propagation velocity, V_{island}/V_{*e}.

TABLE I. Model of $\Delta_{\rm pol}$.

Cold ion $T_i = 0$			
W	$A(W)$	u_+	u_-
3.5	0.0095	1.2	−1.9
6.9	0.0014	1.45	−2.7
9.8	0.0010	1.2	−1.6
Hot ion			
W	A(W)	u_+	u_-
3.5	0.0075	1.3	−5.8
6.9	0.012	−0.3	−9
9.8	0.022	−0.5	−9.5

A. Propagation velocity of magnetic island

A fundamental process in the context of island propagation, as well as for plasma confinement more generally, is the flattening of the density due to the sound wave. The ratio of the sound wave speed to diamagnetic velocity is $c_s/V_{*e} = \sqrt{(\tau_i + 1)}WL_n/(L_s/\epsilon)$. Scott *et al.*[32] have shown that W_c, the island width such that the propagation velocity is reduced to 80% of V_{*e}, is related linearly to the ratio of the magnetic shear length and the density scale length according to $W_c/\rho_s = A + C(L_s/\epsilon)/L_n$. In cold ion plasmas $C = 0.43$, while $C = 0.41$ in Ref. 36 and $C = 2.4$ in Ref. 32. In hot ion plasmas $C = 0.34$, and the flattening of density profile inside the island separatrix is much stronger than that in cold ion plasmas.

The normalized island propagation velocity $V_{\rm island}/V_{*e}$ is plotted as a function of island width in Fig. 7. In incompressible plasma, this velocity is unity independently of the island width. Due to the larger values of the dissipation parameter used here, we do not find the additional, more slowly propagating roots described in Ref. 17. In cold ion plasmas, the propagating velocity is close unity for small island width, while it decreases as the island width become large, consistent with the effect of density flattening described above.

In hot ion plasmas, by contrast, the results are new and unexpected. A simple argument[1] based only on continuity of the ion velocity and on the trapping of electrons inside the separatrix ("frozen-in" property of the electron fluid) leads to the expectation that the island velocity will vary continuously from the electron to the ion diamagnetic frequency as the density flattening increases. According to this simple argument, $1 - V_{\rm island}/V_{*e}$ should be $1 + T_i/T_e$ times larger for hot ions than for cold ions. Fig. 7, however, shows that $V_{\rm island}/V_{*e}$ decreases significantly faster as a function of W, at least up to $W/\rho_i \simeq 8$. Comparison of our results with those of Refs. 30 and 34 leads to the conclusion that $V_{\rm island}/V_{*e}$ evolves much more slowly for W/ρ_i between 8 and 40, changing direction while remaining small. Refs. 30

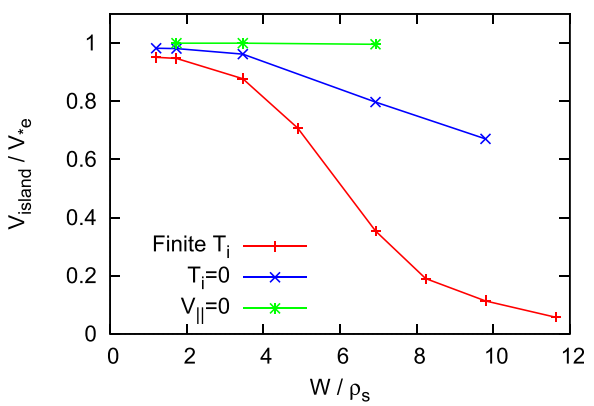

FIG. 7. The propagation velocity of magnetic island V_{island} with $F_y = 0$ in hot ion plasma "Finite T_i"; in cold ion plasma "$T_i = 0$"; in incompressible plasma, "$V_\parallel = 0$."

and 37 account for the large-island results in terms of the Reynolds stress. Unfortunately, the calculation of the effects of the Reynolds stress assumes that the density profile is fully flattened everywhere within the separatrix, a condition that is violated for the more moderately sized islands in our simulations. Thus, our simulations bridge the gap between the thin-island "hypersonic" and the large-island "sonic" regimes described in Ref. 37.

B. Polarization current

We next examine the stability parameter $\Delta_{\rm pol}$, the contribution of the polarization current to island evolution, for freely propagating islands. We evaluate the value of $\Delta_{\rm pol}(u_{\rm free})$ by interpolation from the results in Figs. 1, 3, and 5. Figure 8 shows $\Delta_{\rm pol}$ as a function of the island width W for hot ion plasmas, cold ion plasmas, and incompressible plasmas.

We first describe the incompressible and cold ion cases, where our results are consistent with previous studies. In incompressible plasma, the polarization term vanishes because the island propagation velocity is the electron diamagnetic velocity. In cold ion plasmas, by contrast, $\Delta_{\rm pol}$ is negative, i.e., the polarization term is stabilizing, as shown in Ref. 36. The stabilizing effect peaks near the sound resonance, at $W \sim \rho_s L_s/L_n \sim 3\rho_s$.

We now turn to the case of islands in a quiescent plasma with hot ions. Aside from the large size of $\Delta_{\rm pol}$ already noted in Sec. III C, the results reveal a new surprise: The sign of $\Delta_{\rm pol}$ changes with the island width, and thus the polarization current is *destabilizing* for $W > 5\rho_s$. Hence, the polarization current can drive tearing mode growth even in the absence of bootstrap current, provided that a sufficiently large "seed island" is present.

The circumstances leading to the reversal of the role of the polarization current for large islands are illustrated by Fig. 9 showing the roots $u_\pm$ of $\Delta_{\rm pol}(u_\pm) = 0$ in addition to $u_{\rm free}$. This figure shows that with increasing W, the domain where $\Delta_{\rm pol}$ is stabilizing shifts towards the ion direction faster than the propagation velocity, so that the line of $u_{\rm free}$ crosses that of u_+ around $W = 5\rho_s$, coincident with the marginal point $\Delta_{\rm pol} = 0$ in Fig. 8. Note that for $W > 6\rho_s$, the lower bound of the stable domain, u_-, is obtained by extrapolation of the results shown in Fig. 5.

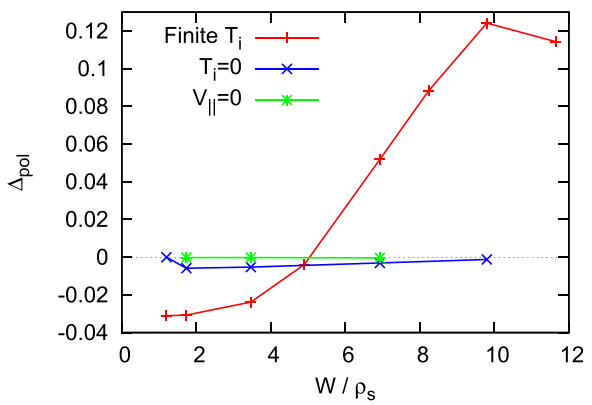

FIG. 8. The polarization current term $\Delta_{\rm pol}$ for magnetic island propagating with its natural velocity V_{island} in compressible plasma with hot ions, "Finite T_i"; in compressible plasma with cold ions, "$T_i = 0$"; in incompressible plasma, "$V_\parallel = 0$."

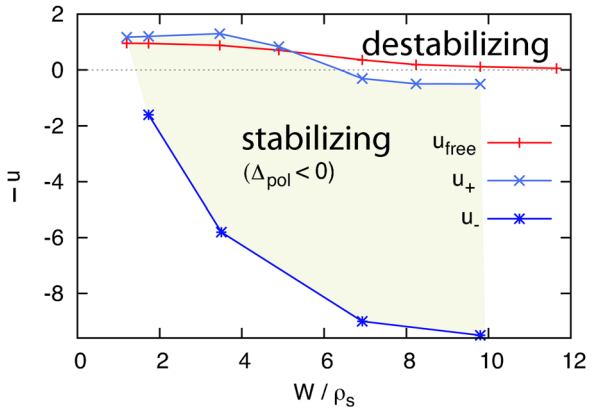

FIG. 9. The root $u_{\rm free}$ of $F_y(u_{\rm free}) = 0$ and the roots u of $\Delta_{\rm pol}(u) = 0$ in Fig. 5 as a function of island width W in hot ion plasmas.

The strength of the destabilizing effect depends on plasma resistivity and viscosity. We briefly describe the dependence on them for $W = 6.9\rho_s$. When we halve the resistivity, the $\Delta_{\rm pol}$ become about 2.5 times larger, on the other hand, when we halve the viscosity, the $\Delta_{\rm pol}$ become 1/3 times smaller approximately. When we halve both of the resistivity and viscosity, the $\Delta_{\rm pol}$ become 3 times larger.

C. Velocity profiles

Some insight into the physics of island propagation in inhomogeneous plasma can be gained by examining the streamlines for electrons and ions. Figure 10(a) shows electron flow streamlines, which are the equi-contours of the electron stream function, $\Phi - n$, in hot ion plasmas for $W/\rho_s = 6.9$. The electron flow pattern is close to the magnetic surfaces, and the electron fluid is well tied to magnetic field lines. Figures 10(b) and 10(c) show ion stream lines, which are the equi-contours of the ion stream function $\Phi + p_i$ in hot ion plasmas for $W/\rho_s = 6.9$ and 9.8, respectively. The stream lines deviate from the magnetic surfaces because of drifts and viscosity. When the island width is much larger than the Larmor radius, the stream lines are close to the magnetic surfaces and the ion fluid is trapped inside the separatrix. This is the result of the "magnetization" of the ion flow with respect to the *perturbed* field. For $W/\rho_s = 9.8$, a pair of small convection cells appears around the O-point, indicating the presence of a standing drift-acoustic wave.

Figure 11 shows the electron flow velocity profiles on the line passing through the O-point of two magnetic islands in hot ion plasmas with $W/\rho_s = 3.5$ and 6.9. Within the island separatrix, the velocity is very small as the electron fluid is trapped within the separatrix. Outside the separatrix, by contrast, the velocity is finite and pointed in the electron diamagnetic direction. There is thus strong shear in the electron flow velocity at the separatrix. The electron flow is enhanced just outside the separatrix (indicated by the vertical lines) on either side of the O-point because the density profile is steepened there. The electron velocity profiles in cold and hot ion plasmas are similar.

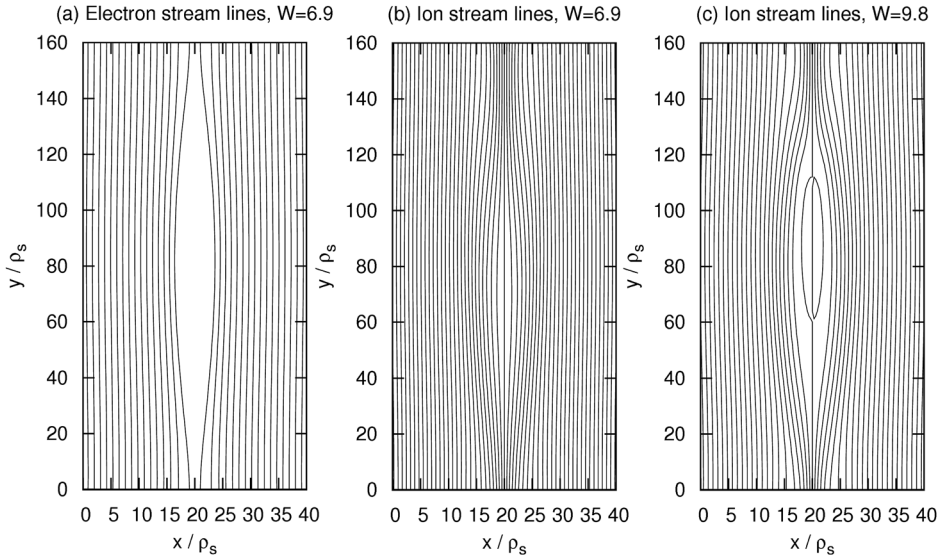

FIG. 10. (a) Electron stream lines with $W/\rho_s = 6.9$; (b) and (c) ion stream lines with $W/\rho_s = 6.9$ and 9.8 for finite T_i plasma.

Figure 12 shows (a) the total ion velocity profiles $V_{iy} = V_{Ey} + V_{diy}$, (b) the E × B electric drift velocity profiles V_{Ey}, and the contributions of (c) the density gradients $V_{dNy} = \partial_x n$ and (d) the temperature gradients $V_{dTy} = \partial_x T_i$ to the ion diamagnetic drift $V_{diy} = V_{dNy} + V_{dTy}$ on the line passing through the O-point of the magnetic island for $W/\rho_s = 3.5$, 6.9, and 9.8. The total ion velocity is always negative and directed toward the negative y direction, which is the ion diamagnetic direction, except for $W = 9.8$ around the O-point at $x = 20\rho_s$ (this is a consequence of the convection cells noted above). For $W/\rho_s = 3.5$, 6.9, the amplitude of total ion velocity is finite both inside and outside the separatrix, because the ion viscosity is much larger than the electron viscosity. The total ion velocity profile has a "W" shape, because the density is flattened within the separatrix as shown in the density-gradient profile, Fig. 12(c), while it is steepened just outside the separatrix. The total ion velocity profile is similar to the reverse of the total electron velocity profile because of opposite electron and ion diamagnetic directions. The profile of the total ion velocity is much smoother than that of the electron velocity because of the larger ion viscosity. The peak of the "W" shape becomes large when the island width is large because of the broadening of the flattening of the density profile. When the width is large enough, we have convection cells within the separatrix for $W/\rho_s = 9.8$.

The profiles in Fig. 12 provide more detailed perspective on the question of why Δ_{pol} in hot ion plasma is much larger than that in cold ion plasma. The polarization current is caused by E × B and ion-diamagnetic convection in the vorticity equation (3), and thus both the total ion velocity shear and the E × B velocity shear contribute. In Figs. 12(a) and 12(b), the total ion velocity and E × B velocity profiles of hot ion plasmas are strongly sheared around the separatrix which is indicated by the vertical lines, while in cold ion plasmas (Figs. 12(e) and 12(f)), these profiles exhibit little shear. We remark that total ion velocity is the same as the E × B velocity in cold ion plasmas, $V_{iy} = V_{Ey}$. The strong velocity shear is supported by the Maxwell stress as shown in Fig. 13. The figure shows the profile of each term in the vorticity equation on the line passing through the O-point of the magnetic island $y = L_y/2$ for $W/\rho_s = 6.9$. The viscosity term, that suppress the shear, is large around the separatrix. The Maxwell stress term is large and counteracts the suppression of flow shear by viscosity term, while the Reynolds stress and ion diamagnetic stress terms are small. Thus, the large viscosity term due to the strong velocity shear balances with the Maxwell stress term.

D. Current density profiles

Figure 14 shows a color map of the perturbed part of the current density for $W/\rho_s = 3.5$ and 6.9. The bold line in the figure shows the magnetic island separatrix. Note that the asymmetry of the current with respect to the y direction is caused by the viscous force on the island, which induces a parallel current proportional to $\sin(k_{y1}y)$. This current does

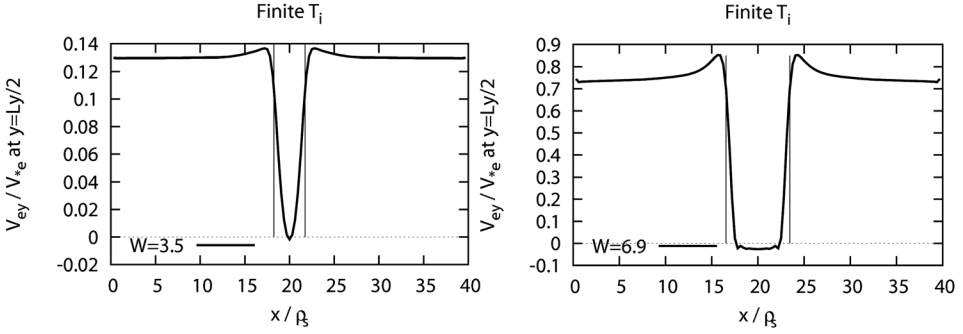

FIG. 11. Electron velocity profile on the line passing through the O-point $y = L_y/2$ for finite T_i plasma with $F_y = 0$ and $W/\rho_s = 3.5$ and 6.9. Vertical lines indicate the separatrix of magnetic island.

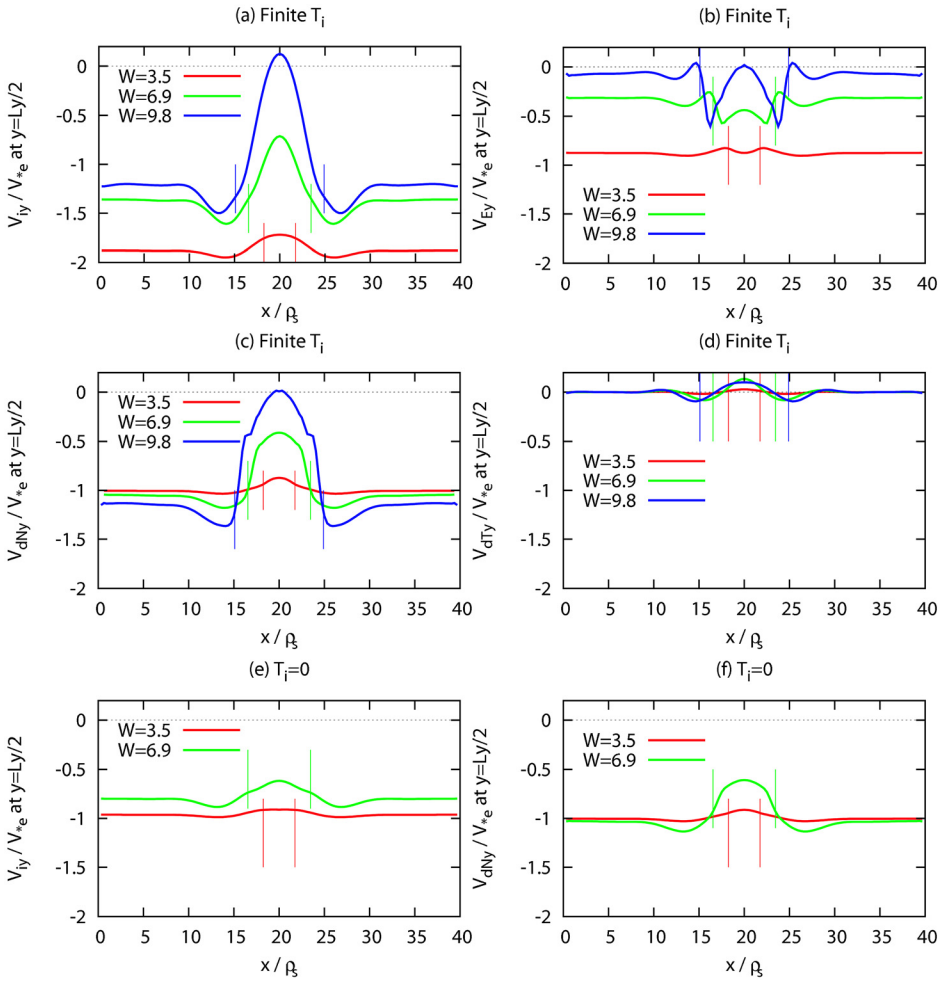

FIG. 12. (a) Ion velocity $V_{iy} = V_{Ey} + V_{dNy} + V_{dTy}$, (b) E × B velocity V_{Ey}, (c) density diamagnetic velocity V_{dNy}, and (d) ion temperature diamagnetic velocity V_{dTy} for finite T_i plasma, and (e) V_{iy} and (f) V_{dNy} for $T_i = 0$ plasma on the line passing through the O-point $y = L_y/2$ with $F_y = 0$ and $W/\rho_s = 3.5$, 6.9, and 9.8. Vertical lines indicate the separatrix.

not contribute to the polarization integral Δ_{pol}, which contains only the $\cos(k_{y1}y)$ component of the current caused by ion inertia.

For $W/\rho_s = 3.5$ the current density is negative and large around the separatrix in the lower half of the frame. In the upper half of the frame, the strong negative current density region is located outside of the separatrix of the island, and it is positive and large around the X-point. The strong current density in the upper half of the frame dominates the contribution to the polarization current term and makes it negative: $\Delta_{\mathrm{pol}} \propto -\int J \cos k_{y1} y dx dy < 0$.

For $W/\rho_s = 6.9$, the current density is large not only around the separatrix but within the separatrix of island. In the lower half of the frame, $-J \cos k_{y1} y$ is largely positive within the separatrix, and this positive contribution

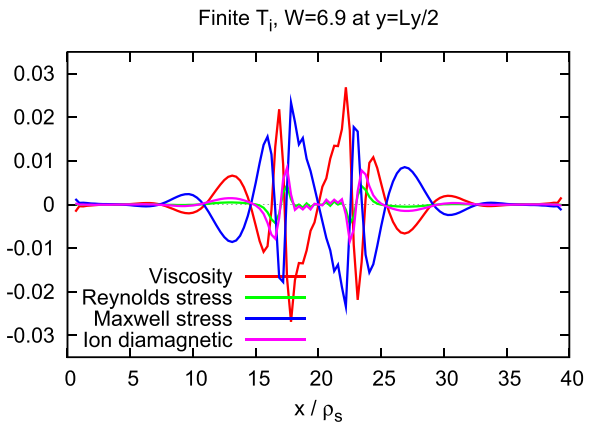

FIG. 13. Profile of each term in the vorticity equation on the line passing through the O-point $y = L_y/2$ for finite T_i plasma with $F_y = 0$ and $W/\rho_s = 6.9$.

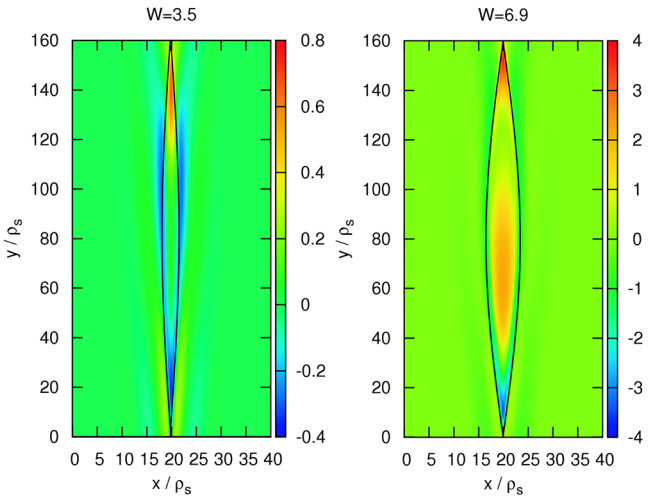

FIG. 14. Color map of current density for finite T_i plasma with $F_y = 0$ and $W/\rho_s = 3.5$ and 6.9. Solid lines indicate the separatrix.

dominates the polarization current integral and leads to $\Delta_{\rm pol} \propto -\int J \cos k_{y1} y dx dy > 0$.

V. SUMMARY

We have carried out numerical simulations of a reduced set of two-fluid equations including both electron and ion diamagnetic effects as well as ion temperature evolution, and presented effects of finite ion temperature on the propagation velocity of magnetic island and on the polarization current.

We find that the magnetic island propagates toward the electron diamagnetic direction for island of widths up to 10 times the Larmor radius. As the width of a magnetic island in a hot-ion plasma increases, its propagation velocity slows down much faster than in a cold-ion plasma. In hot-ion plasma, the propagation velocity of large islands is small compared to the diamagnetic velocities.

We also find that when the island width is larger than $5\rho_s$, the polarization current $\Delta_{\rm pol}$ becomes *destabilizing* in hot ion plasmas. The critical width $W_c \approx 5\rho_s$ is determined by the change in island propagation velocity with the island width. The destabilization is the strongest when the island width is about $10\rho_s$. This destabilizing effect of $\Delta_{\rm pol}$ in finite ion temperature is important because the threshold of NTM excitation is several times of ion Larmor radius.[4] The destabilization is in contrast with the stabilizing effect of the polarization current for thinner islands and in cold ion plasmas. Lastly, we find that the polarization current in hot ion plasma is about ten times larger than that in cold ion plasmas. Such large polarization current in hot ion plasma is produced by strong velocity shear around the separatrix of the magnetic island. The velocity shear is driven by the Maxwell stress, while it is balanced primarily by the viscous stress.

ACKNOWLEDGMENTS

The work is supported by Joint Institute for Fusion Theory exchange program, by the Japanese Ministry of Education, Culture, Sports, Science and Technology, Grant No. 23561003, and by the U.S. DOE under Grant No. DE-FG02-04ER-54742. One of the authors A.I. would like to thank Professor R. Horiuchi and Professor H. Sugama for their support.

[1]F. L. Waelbroeck, "Theory and observations of magnetic islands," Nucl. Fusion **49**(10), 104025 (2009).
[2]P. H. Rutherford, "Nonlinear growth of the tearing mode," Phys. Fluids **16**(11), 1903 (1973).
[3]R. J. La Haye, "Neoclassical tearing modes and their control," Phys. Plasmas **13**(5), 055501 (2006).
[4]R. J. La Haye and O. Sauter, "Threshold for metastable tearing modes in DIII-D," Nucl. Fusion **38**(7), 987–999 (1998).
[5]R. J. Buttery, R. Akers, E. Arends, N. J. Conway, G. F. Counsell, G. Cunningham, C. G. Gimblett, M. Gryaznevich, R. J. Hastie, M. J. Hole, I. Lehane, R. Martin, A. Patel, T. Pinfold, O. Sauter, D. Taylor, G. Turri, M. Valovic, M. J. Walsh, H. R. Wilson, and the MAST Team, "Stability at high performance in the MAST spherical tokamak," Nucl. Fusion **44**(9), 1027–1035 (2004).
[6]I. T. Chapman, V. G. Igochine, J. P. Graves, S. D. Pinches, A. Gude, I. Jenkins, M. Maraschek, G. Tardini, the ASDEX Upgrade Team, and JET EFDA Contributors, "Sawtooth control and the interaction of energetic particles," Nucl. Fusion **49**(3), 035006 (2009).
[7]H. Zohm, "Stabilization of neoclassical tearing modes by electron cyclotron current drive," Phys. Plasmas **4**(9), 3433–3435 (1997).
[8]G. Gantenbein, H. Zohm, G. Giruzzi, S. Günter, F. Leuterer, M. Maraschek, J. Meskat, Q. Yu, ASDEX Upgrade Team, and ECRH-Group (AUG), "Complete suppression of neoclassical tearing modes with current drive at the electron-cyclotron-resonance frequency in ASDEX upgrade tokamak," Phys. Rev. Lett. **85**(6), 1242–1245 (2000).
[9]A. Isayama, Y. Kamada, T. Ozeki, S. Ide, T. Fujita, T. Oikawa, T. Suzuki, Y. Neyatani, N. Isei, K. Hamamatsu, Y. Ikeda, K. Takahashi, K. Kajiwara, and JT-60 Team, "Long sustainment of quasi-steady-state high β_p h mode discharges in JT-60U," Nucl. Fusion **41**(6), 761–768 (2001).
[10]E. Westerhof, A. Lazaros, E. Farshi, M. R. de Baar, M. F. M. de Bock, I. G. J. Classen, R. J. E. Jaspers, G. M. D. Hogeweij, H. R. Koslowski, A. Krämer-Flecken, Y. Liang, N. J. Lopes Cardozo, and O. Zimmermann, "Tearing mode stabilization by electron cyclotron resonance heating demonstrated in the TEXTOR tokamak and the implication for ITER," Nucl. Fusion **47**(2), 85–90 (2007).
[11]C. C. Hegna and J. D. Callen, "On the stabilization of neoclassical magnetohydrodynamic tearing modes using localized current drive or heating," Phys. Plasmas **4**(8), 2940–2946 (1997).
[12]L. Urso, H. Zohm, A. Isayama, M. Maraschek, E. Poli, ASDEX Upgrade Team, and JT-60 Team, "ASDEX upgrade—JT-60U comparison and ECRH power requirements for NTM stabilization in ITER," Nucl. Fusion **50**(2), 025010 (2010).
[13]A. Gude, S. Günter, S. Sesnic, and ASDEX Upgrade Team, "Seed island of neoclassical tearing modes at ASDEX upgrade," Nucl. Fusion **39**(1), 127–131 (1999).
[14]E. D. Fredrickson, "Observation of spontaneous neoclassical tearing modes," Phys. Plasmas **9**(2), 548–559 (2002).
[15]S.-I. Itoh, K. Itoh, and M. Yagi, "Turbulence trigger for neoclassical tearing modes in tokamaks," Plasma Phys. Controlled Fusion **46**(1), 123–143 (2004).
[16]F. Militello, F. L. Waelbroeck, R. Fitzpatrick, and W. Horton, "Interaction between turbulence and a nonlinear tearing mode in the low beta regime," Phys. Plasmas **15**(5), 050701 (2008).
[17]F. L. Waelbroeck, F. Militello, R. Fitzpatrick, and W. Horton, "Effect of electrostatic turbulence on magnetic islands," Plasma Phys. Controlled Fusion **51**(1), 015015 (2009).
[18]A. Ishizawa and N. Nakajima, "Turbulence driven magnetic reconnection causing long-wavelength magnetic islands," Phys. Plasmas **17**(7), 072308 (2010).
[19]M. Muraglia, O. Agullo, S. Benkadda, M. Yagi, X. Garbet, and A. Sen, "Generation and amplification of magnetic islands by drift interchange turbulence," Phys. Rev. Lett. **107**, 095003 (2011).
[20]H. R. Wilson and J. W. Connor, "The influence of magnetic islands on drift mode stability in magnetized plasma," Plasma Phys. Controlled Fusion **51**(11), 115007 (2009).
[21]A. Ishizawa and P. H. Diamond, "Ion-temperature gradient modes affected by helical magnetic field of magnetic islands," Phys. Plasmas **17**(7), 074503 (2010).
[22]Z. X. Wang, J. Q. Li, Y. Kishimoto, and J. Q. Dong, "Magnetic-island-induced ion temperature gradient mode," Phys. Plasmas **16**(6), 060703 (2009).
[23]A. I. Smolyakov, "Nonlinear evolution of tearing modes in inhomogeneous plasmas," Plasma Phys. Controlled Fusion **35**, 657 (1993).
[24]R. Fitzpatrick, "Interaction of tearing modes with external structures in cylindrical geometry," Nucl. Fusion **33**, 1049–1084 (1993).
[25]F. L. Waelbroeck, J. W. Connor, and H. R. Wilson, "Finite larmor-radius theory of magnetic island evolution," Phys. Rev. Lett. **87**, 215003 (2001).
[26]E. Poli, A. Bergmann, A. G. Peeters, L. C. Appel, and S. D. Pinches, "Kinetic calculation of the polarization current in the presence of a neoclassical tearing mode," Nucl. Fusion **45**(5), 384–390 (2005).
[27]F. L. Waelbroeck and R. Fitzpatrick, "Rotation and locking of magnetic islands," Phys. Rev. Lett. **78**, 1703–1706 (1997).
[28]R. Fitzpatrick and F. L. Waelbroeck, "Two-fluid magnetic island dynamics in slab geometry. I. Isolated islands," Phys. Plasmas **12**(2), 022307 (2005).
[29]R. Fitzpatrick and F. L. Waelbroeck, "Two-fluid magnetic island dynamics in slab geometry. II. Islands interacting with resistive walls or resonant magnetic perturbations," Phys. Plasmas **12**(2), 022308 (2005).

[30]R. Fitzpatrick, P. Watson, and F. L. Waelbroeck, "Two-fluid magnetic island dynamics in slab geometry: Determination of the island phase velocity," Phys. Plasmas **12**(8), 082510 (2005).
[31]R. Fitzpatrick and F. L. Waelbroeck, "Effect of drift-acoustic waves on magnetic island stability in slab geometry," Phys. Plasmas **12**(12), 122511 (2005).
[32]B. D. Scott, A. B. Hassam, and J. F. Drake, "Nonlinear evolution of drift-tearing modes," Phys. Fluids **28**(1), 275 (1985).
[33]R. J. La Haye, C. C. Petty, E. J. Strait, F. L. Waelbroeck, and H. R. Wilson, "Propagation of magnetic islands in the $e_r = 0$ frame of co-injected neutral beam driven discharges in the DIII-D tokamak," Phys. Plasmas **10**(9), 3644–3648 (2003).
[34]K. Uzawa, A. Ishizawa, and N. Nakajima, "Propagation of magnetic island due to self-induced zonal flow," Phys. Plasmas **17**(4), 042508 (2010).
[35]A. Ishizawa and N. Nakajima, "Excitation of macromagnetohydrodynamic mode due to multiscale interaction in a quasi-steady equilibrium formed by a balance between microturbulence and zonal flow," Phys. Plasmas **14**(4), 040702 (2007).
[36]R. Fitzpatrick, F. L. Waelbroeck, and F. Militello, "The influence of the ion polarization current on magnetic island stability in a tokamak plasma," Phys. Plasmas **13**(12), 122507 (2006).
[37]R. Fitzpatrick and F. L. Waelbroeck, "Drift-tearing magnetic islands in tokamak plasmas," Phys. Plasmas **15**(1), 012502 (2008).